Physical Chemistry Chemical Physics. 1999, 1, 3667 - 3671

PCCP

# Lag phases in the adsorption of lysozyme to $Si(Ti)O_2$ surfaces in the presence of sodium thiocyanate

## Part I. Phenomenology

**Vincent Ball,*† Ariel Lustig and Jeremy J. Ramsden**

*Department of Biophysical Chemistry, Biocentre of the University, Klingelbergstrasse 70, CH-4056 Basel, Switzerland*

***Received 23rd April 1999, Accepted 9th June 1999***

The adsorption kinetics of hen egg white lysozyme (HEWL) in the presence of NaSCN at pH 7.4 onto $Si_{0.8}Ti_{0.2}O_2$ surfaces were measured by means of time-resolved optical waveguide lightmode spectroscopy (OWLS). The adsorption kinetics were characterized by the presence of a lag phase whose duration decreased with increasing lysozyme bulk concentration. This lag phase was followed by rapid growth of the interfacial protein film which ceased at a surface coverage close to that predicted for a monolayer. At bulk concentrations lower than about 50 μg $cm^{-3}$, the maximum rate of adsorption was equal to the rate predicted for a transport-controlled process from the solution to the surface and at higher bulk concentrations such lag phases were no longer observed. Storage of lysozyme solution prior to adsorption reduced the duration of the lag phase, but analytical ultracentrifugation measurements showed the absence of significant aggregation even at bulk concentrations of $10^3$ μg $cm^{-3}$. These features are consistent with an adsorption process requiring the adsorption of a small critical nucleus preformed in solution followed by the completion of the adlayer by a mechanism akin to crystal growth. The size of this critical nucleus was estimated to be of the order of only a few lysozyme molecules.

## Introduction

The adsorption of hen egg white lysozyme (HEWL) at the solid/liquid interface presents some unusual features.[1] At low ionic strength, the observation of the absence of the usual effects of excluded area[2] was taken to imply the formation of one-dimensional aggregates at the surface. The predicted existence of these aggregates was later confirmed by direct observation in the atomic force microscope.[3]

Electrostatic potential calculations on the surface of the HEWL molecule suggest that this self-association process, mediated by the presence of the surface, is related to the asymmetry of the charge distribution and the corresponding large dipole moment of about 70 D‡ at pH 7.0.[4] Our previous results[1] are also consistent with observations of lysozyme self-aggregation in bulk solution under certain conditions.[5–7]

Although ionic strength effects on protein adsorption kinetics have been previously examined,[8] investigators have generally confined themselves to the most common salt, NaCl. Indeed, one of the few comparative experiments (on serum albumin[9]) showed very significant differences between adsorption on silica–titania in the presence of either phosphate (a kosmotropic salt[10,11]) and NaCl. The significant difference observed between the adsorption of lysozyme and chymotrypsinogen A on butylated and aminopropylated quartz surfaces at pH 7.0 in the presence of either NaCl or $(NH_4)_2SO_4$ (also a kosmotrope)[12,13] was attributed to a modification of the interfacial tension of the protein/solution interface.

Here we report our finding that HEWL adsorption on an amorphous silica–titania surface in the presence of the strongly chaotropic salt, NaSCN,[10,11] differs even more from the behaviour observed in the presence of NaCl. The adsorption was followed in real time by means of optical waveguide lightmode spectroscopy (OWLS), a technique which enables protein surface concentration to be measured with an accuracy of a few ng $cm^{-2}$.[14]

## Experimental

### Buffer solutions

Hepes [*N*-(2-hydroxyethyl)piperazine-*N*′-(2-ethanesulfonic acid)] was purchased from Sigma. NaCl (Merck) and NaSCN (Fluka) were both of analytical grade. All solutions were prepared from Nanopure water (resistivity >17.8 MΩ cm). The pH was adjusted to 7.4 by means of freshly prepared 1.0 M NaOH solutions and checked by means of a calibrated glass electrode (Inlab 422, Mettler Toledo, Switzerland).

Hepes has a p$K_a$ of 7.5 at 298 K and is thus 44.3% dissociated at pH 7.4. Hence the concentration of dissociated molecules is $4.43 \times 10^{-3}$ M in $10^{-2}$ M buffer. By assuming that only the free ions and not the zwitterionic molecules contribute to the screening of the electrostatic interactions, the Debye screening length is 2.53 nm (if all Hepes molecules contribute equally to the electrostatic screening, whether in the dissociated or zwitterionic form, then the Debye length is 2.15 nm). Therefore, the range of electrostatic interactions is close to the molecular dimensions of HEWL ($4.5 \times 3.0 \times 3.0$ $nm^3$).[15]

### Protein solutions

HEWL from Sigma (ref. L-6876, lot 65H7025) was used without further purification. If not otherwise stated, concentrated mother protein solutions (about $10^4$ μg $cm^{-3}$ in buffer, $10^{-2}$ M Hepes $+10^{-2}$ M 1 : 1 electrolyte) were prepared shortly before the beginning of an adsorption experiment, diluted to the desired concentration about 10 min later, and introduced into the OWLS cell after a further 10 min.

† Present address: Laboratoire de spectrométrie de masse bio-organique, CNRS UMR 75-09, Institut de Chimie, 1 rue Blaise Pascal, 67008 Strasbourg Cédex, France. E-mail: vball@chimie.u-strasbg.fr

‡ 1 D (debye) ≈ $3.335\,64 \times 10^{-30}$ C m.

**Table 1** Summary of the essential results obtained during the HEWL adsorption experiments on $Si_{0.8}Ti_{0.2}O_2$ surfaces in presence of Hepes-NaSCN buffer

| Chip[a] | $d_F$/nm and $n_F$[b] | $T$ (±0.01)/K | $C_B$/μg cm$^{-3}$ | $t^*$/s[d] | $J^*$/μg cm$^{-2}$ s$^{-1}$ [e] | $\Gamma^*$/μg cm$^{-2}$ [f] | $n^*$ [g] |
|---|---|---|---|---|---|---|---|
| 1 | 177.71, 1.76340 | 298.9 | 1.0 | 5300–5600 | $8.5 \pm 0.1 \times 10^{-5}$ | $0.11 \pm 0.01$ | 1.8 |
| 1 | 177.79, 1.76226 | 298.2 | 2.0 | 3800–3900 | $1.9 \pm 0.1 \times 10^{-4}$ | $0.12 \pm 0.01$ | 1.9 |
| 1 | 175.89, 1.76141 | 296.9 | 5.0 | 2800–2850 | $3.6 \pm 0.1 \times 10^{-4}$ | $0.12 \pm 0.01$ | 2.0 |
| 1 | 177.48, 1.76307 | 299.1 | 10.0 | 1075–1125 | $4.5 \pm 0.2 \times 10^{-4}$ | $0.10 \pm 0.02$ | 2.1 |
| 2 | 205.21, 1.76404 | 301.3 | 15.0 | 900–940 | $5.3 \pm 0.2 \times 10^{-4}$ | $0.10 \pm 0.01$ | 2.2 |
| 1 | 176.30, 1.76109 | 300.1 | 20.0 | 675–725 | $7.5 \pm 1.0 \times 10^{-4}$ | $0.12 \pm 0.02$ | 2.2 |
| 2 | 205.63, 1.76413 | 301.1 | 30.0 | 300–350 | $1.3 \pm 0.3 \times 10^{-3}$ | $0.11 \pm 0.02$ | 2.2 |
| 2 | 205.57, 1.76373 | 298.1 | 52.5 | 500–550 | $1.8 \pm 0.2 \times 10^{-3}$ | $0.12 \pm 0.02$ | 2.3 |
| 1 | 175.07, 1.76095 | 299.5 | 100.4 | 75–125 | $2.9 \pm 0.2 \times 10^{-3}$ | $0.12 \pm 0.05$ | 2.5 |
| 1 | 174.67, 1.76073 | 298.9 | 167.0 | 180–220 | $3.1 \pm 1.0 \times 10^{-3}$ | $0.12 \pm 0.05$ | 2.6 |

[a] Two different type 2400 chips were used in this study, to evaluate the reproducibility from chip to chip. [b] Thickness, $d_F$, and refractive index, $n_F$, of the oxide layer. [c] Temperature at which protein adsorption was measured. [d] Time ellapsed after the beginning of protein injection in the adsorption cell at which the maximal adsorption rate was measured. [e] Value of the maximal adsorption rate at time $t^*$. [f] Surface concentration in adsorbed HEWL at time $t^*$. [g] Size of the critical nucleus calculated with the values of $\Gamma^*$ and $J^*$ and eqn. (3).

Since lysozyme is known to crystallize at relatively low concentrations in the presence of thiocyanate ions at pH 4.5 and 291 K,[16,17] we checked the association state at pH 7.4 using analytical ultracentrifugation[18] (sedimentation velocity (SV) and sedimentation equilibrium (SE) runs in a Beckman model XLA analytical ultracentrifuge equipped with an optical absorption system). The SV runs were carried out in 1.2 cm epon cells at 293 K and $5.6 \times 10^4$ rotations per minute (giving an acceleration of about $2.4 \times 10^5$ g) and SE experiments were performed at the same temperature at $3.0 \times 10^4$ rpm (giving about $7 \times 10^4$ g) in a laboratory-made 0.4 cm DS cell. The reason for using two different kinds of cells is to ensure approximately the same absorbance in both SE and SV experiments. The HEWL solution ($9.7 \times 10^2$ μg cm$^{-3}$) was prepared about 12 h before the beginning of the centrifugation experiments which themselves lasted 12 to 16 h, *i.e.* far longer than the duration of an adsorption experiment. Protein aggregation in solution, if it occurs, is therefore liable to be overestimated. Mean molecular weights were determined by fitting the logarithm of the absorbance at 280 nm *vs.* the square of the radial distance from the rotation axis. We used a value of 0.72 cm$^3$ g$^{-1}$ for the partial specific volume of HEWL[19] in agreement with the value derived from X-ray diffraction data.[20] The sedimentation coefficients at 20 °C, $S_{20,w}$, are $1.56 \times 10^{-13}$ s and $1.61 \times 10^{-13}$ s for $10^{-2}$ M NaCl and NaSCN in Hepes buffer respectively.

The average molecular weight derived from the ultracentrifugation experiment $1.40 \times 10^4$ and $1.39 \times 10^4$ g mol$^{-1}$ in NaSCN and NaCl respectively is close to that calculated from the amino acid sequence (14305 g mol$^{-1}$ when the four disulfide bridges are formed) and there is no significant difference between the two electrolytes. Hence we conclude that at this concentration of NaSCN, HEWL is in the same aggregation state as in the presence of NaCl, *i.e.* mainly in the monomeric form. Note, however, that the solutions used for the ultracentrifugation experiments were about 10 times less concentrated than the mother solutions subsequently diluted for the adsorption experiments. Although this high concentration might play a rôle in promoting aggregation, it is probably negligible since this very concentrated protein solution was aged for only 10 min and then diluted at least 70 times, upon which any preformed aggregates would redissolve. No sedimentation cells thin enough to allow use of the same concentrations as those used for the preparation of the adsorption mother solutions were available.

The refractive index increment d$n$/d$c$ of lysozyme whose value is necessary for a precise calculation of the surface concentration, has been measured by means of Rayleigh interferometry (LI3 interferometer, Carl Zeiss, Jena).[21] In Hepes buffer containing $10^{-2}$ M NaSCN, the refractive index increment, 0.272 cm$^3$ g$^{-1}$, is significantly higher than the 0.186 cm$^3$ g$^{-1}$ measured in presence of $10^{-2}$ M NaCl.

### Surface cleaning and characterization

Planar optical waveguides consist of a thin and amorphous sol–gel[22] $SiO_2$–$TiO_2$ oxide layer coated onto 48 × 16 × 0.5 mm Schott Desag AF45 glass substrates (refractive index $n_S$ = 1.52578 at 298 K and at 632.8 nm). $TiO_2$ is present in the film as anatase as demonstrated by Raman spectroscopy.[23] A 2 mm wide diffraction grating with a periodicity of 2403 mm$^{-1}$ was produced by embossing before pyrolysis of the sol–gel oxide layer.[22] The assembly of the glass substrate and the mixed oxide with its grating coupler constitutes a chip. These chips were cleaned with ethanol, Nanopure water, $10^{-2}$ M SDS (sodium dodecyl sulfate) solutions at 80 °C for about 10 min, again Nanopure water, 0.1 M HCl at 80 °C for 10 min, extensively rinsed with Nanopure water and finally equilibrated in buffer for at least 2 h.

## OWLS

The chips were mounted beneath and sealed to an anodized aluminium flow-through cuvette with a perfluorinated o-ring (Kalrez®, Dupont), which in turn was mounted in an IOS-1 integrated optics scanner (Artificial Sensing Instruments, Zürich).[24] Deaerated buffer, filtered through 0.2 μm pore diameter Millisart membranes (Sartorius), flowed over the surface until the baseline was stable (drift of the effective refractive index lower than $10^{-6}$ min$^{-1}$). Freshly prepared protein solution then flowed through the same type of filter at a constant rate of 2.46 μl s$^{-1}$ (checked by weighing), corresponding to a wall shear rate and Reynolds number of 16.6

$s^{-1}$ and 0.3 respectively *i.e.* laminar flow with a diffusion boundary layer 234 μm thick.[1]

At the end of each experiment, the flow was switched back to protein-free buffer to allow protein desorption to be monitored. Finally, the chip was removed and cleaned as described above.

Temperature was monitored by means of a Pt-100 resistance localized in the aluminium sample holder close to the chip. All experiments (Table 1) took place within the temperature range 297–301 K, but within an individual experiment temperature fluctuations were controlled within $\pm 0.1$ K. The zeroth transverse electric and transverse magnetic effective refractive indices were continuously recorded during all stages of each experiment.

The thickness $d_F$ and the refractive index $n_F$ of the oxide layer were evaluated by fitting a three layer model[25] to the effective refractive indices obtained in the steady response régime during initial buffer equilibration. The reproducibility of our cleaning method was checked by comparing ($d_F$, $n_F$) values from experiment to experiment (Table 1) We observed a sudden decrease in $d_F$ and a concomitant increase in $n_F$ after 7 to 10 experimental cycles, possibly due to acid induced surface etching. We stopped using that chip at that point. As an additional check, a chip previously exposed to protein was cleaned as described, dried in the presence of anhydrous $CuSO_4$, and the central region of the diffraction grating analyzed in air using atomic force microscopy (Nanoscope III, Digital Instruments, Santa Barbara, California). The root mean square roughness of this region was found to be 0.84 nm, relatively small compared with the size of HEWL.[15] Moreover, no trace of any residual protein islands could be detected, indicating quantitative removal of the adsorbed HEWL by our cleaning method.

At a buffer pH of 7.4, the oxide surface is negatively charged (the points of zero charge for pure silica and titania in the anatase form are 2.5 and 5.8 respectively[26,27]) whereas the protein carries a net positive charge of about 8 elementary charges (its isoelectric point is 11.1[15]). At present, we do not know if a highly polarizable anion such as $SCN^-$ adsorbs specifically to the oxide surface. However, strong interactions between the protein and thiocyanate ions have been characterized[28] at neutral pH, probably modifying the surface charge density of HEWL and hence its interactions with the mixed oxide surface.

The number of HEWL molecules adsorbed per unit area of the flat surface was calculated from the measured effective refractive indices as described previously.[29]

## Results and discussion

Typical adsorption kinetics in $10^{-2}$ M NaSCN and $10^{-2}$ M Hepes buffer at pH 7.4 are shown in Fig. 1. The most interesting observation is the occurrence of a reproducible lag phase in the HEWL adsorption kinetics at protein concentrations lower than about 50 μg $cm^{-3}$. The lower the protein concentration in solution, the longer the lag phase (Fig. 1 and Table 1). Its duration can be estimated from the interval between the beginning of protein flow ($t = 0$) and the occurrence of the maximum adsorption rate, (the point of inflexion in the kinetics). At bulk concentrations higher than about 50 μg $cm^{-3}$, the initial adsorption rate becomes so fast that the inflexion point occurs after about 100 to 200 s, not significantly more than the time required for reaching steady state in the formation of the diffusion boundary layer, namely about 120 s.

Moreover, in the lower concentration régime only, we found the maximum adsorption rate to be equal to the rate of diffusive convection of HEWL from the bulk of the solution to the surface (Fig. 1), taking the diffusion coefficient of monomeric HEWL to be $1.04 \times 10^{-6}$ $cm^2$ $s^{-1}$.[15] The observed lag

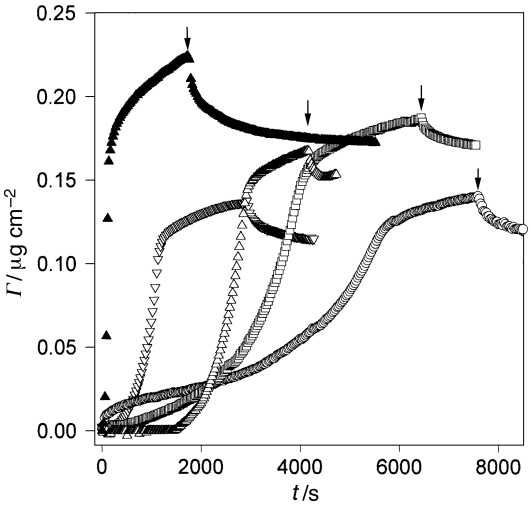


**Fig. 1** Some representative adsorption kinetics of HEWL dissolved in $10^{-2}$ M Hepes buffer with $10^{-2}$ M NaSCN on the $Si_{0.8}Ti_{0.2}O_2$ surface of chip 1. The flow rate was maintained constant at 2.46 μl $s^{-1}$ in all steps of the experiments. On each curve the arrow indicates the switch from the protein solution flow to pure buffer, hence the beginning of the desorption kinetics. Lysozyme bulk concentrations are: 1 (○), 2 (□), 5 (△), 10 (▽) and 100 μg $cm^{-3}$ (▲).

phase suggests that adsorption proceeds *via* nucleation and subsequent growth on the silica–titania surface. At bulk concentrations higher than about 50 μg $cm^{-3}$, a maximum in the adsorption rate appears at very short times (Table 1). At present we do not know if this originates from an hydrodynamic effect or from critical nucleus formation. In any case, the maximal adsorption rates for these higher HEWL concentrations are significantly lower than those predicted for the transport of monomers to the interface (Fig. 2).

The occurrence of a possible nucleation régime in the adsorption kinetics at protein concentrations lower than about 50 μg $cm^{-3}$ is further illustrated by the following experiment: a 10 μg $cm^{-3}$ lysozyme solution was stored after dilution at ambient temperature in a closed glass container of the mother solution. Part of this solution was used as usual 10 min after dilution for an adsorption experiment, and the rest used 3 h later, after which the lag phase duration was much shorter (Fig. 3). This suggests the formation of nuclei *in the bulk solution* before adsorption to the surface. Once a few aggregates are adsorbed, fast adsorption, *i.e.* a kind of crystallization, proceeds. When the preincubation time is shorter, fewer preformed aggregates are present. Let us assume that

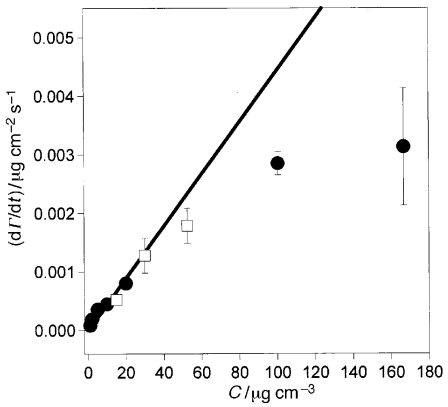


**Fig. 2** Evolution of the maximal adsorption rate with the concentration of dissolved HEWL, as measured at the inflexion points of the adsorption kinetics. Experiments performed with chip 1: ●, and with chip 2: □ (see Table 1). The straight line corresponds to the adsorption rates equal to $Dc_B/\delta$, hence to a kinetic process ruled by convective diffusion, see text for further explanations ($\delta$ is the thickness of the diffusion boundary layer).

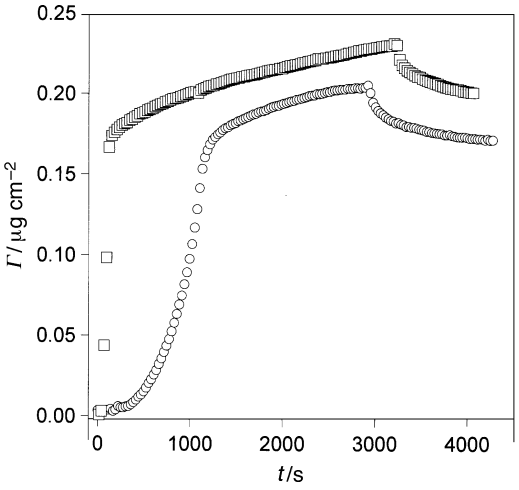


**Fig. 3** Influence of the storage time on the adsorption kinetics of a 10 μg $cm^{-3}$ HEWL solution. Adsorption experiment beginning 10 min (○) and 180 min (□) after its preparation from a mother solution at about $10^4$ μg $cm^{-3}$ (see text).

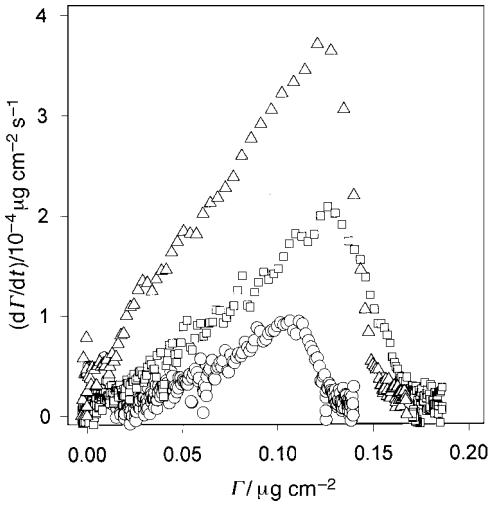


**Fig. 4** Representative curves of the time derivative of the surface concentration of adsorbed HEWL as a function of $\Gamma$, for bulk concentrations of 1 (○), 2 (□) and 5 μg $cm^{-3}$ (△).

the lag phase duration corresponds to the time needed for a critical nucleus to appear on the surface.

According to classical nucleation theory, the maximal growth rate $J^*$ should be related to the free energy activation barrier for the formation of the critical nucleus, $\Delta G^{\neq}$, according to the relation:[30]

$$J^* = \left(\frac{D}{d_A^4}\right)\exp\left(\frac{-\Delta G^{\neq}}{kT}\right) \quad (1)$$

where $d_A$ is the thickness of the adlayer, assumed to be of the order of 4 nm, and $D$ the translational diffusion coefficient of monomers. In addition, $\Delta G^{\neq}$, is related to the supersaturation, $c^*/c_B$, according to:

$$\Delta G^{\neq} = n^* kT \ln\left(\frac{c^*}{c_B}\right) \quad (2)$$

where $n^*$ is the number of molecules in the critical nucleus and $c^*$ the HEWL concentration in the supersaturated film. Combining eqns. (1) and (2), and setting $c^*$ to $\Gamma^*/d_A$, namely the volumetric concentration in the surface film at the inflexion point of the adsorption kinetics (about 0.5 g $cm^{-3}$), one obtains:

$$J^* = \frac{1}{m}\left(\frac{d\Gamma}{dt}\right)_{\Gamma=\Gamma^*} = \left(\frac{D}{d_A^4}\right)\left[\frac{\Gamma^*}{c_B d_A}\right]^{n^*} \quad (3)$$

where $m$ is the mass of an adsorbing monomer. The fact that we normalize the adsorption rate with the mass of a monomer originates from the observation of Fig. 2: the maximal adsorption rate is that corresponding to diffusion–convection of particles mainly in the monomeric state.

Hence the size of the critical nucleus can be calculated from the measured value of the maximum adsorption rate. Taking typical values of $\Gamma^* = 0.12$ μg $cm^{-2}$ (Fig. 4, and Table 1), a maximal adsorption rate of 1.5 ng $cm^{-2}$ $s^{-1}$ (Fig. 4) and $c_B =$ 40 μg $cm^{-3}$, one obtains $n^* \approx 1$ to 3. Values for each individual experiment are listed in Table 1. This n* value appears not to be inconsistent with the results of our ultracentrifugation experiments (see Experimental part): if the concentrated lysozyme solution contained a significant amount *of very big aggregates*, then the mean molecular weight of the sedimenting particles would not have been so close to that of monomeric HEWL. However, we are not able to characterize such small aggregates with ultracentrifugation, but will attempt to do so by means of light scattering in subsequent work.

Bimodal adsorption of bovine serum albumin or human IgG on latex particles from pH 7.4 phosphate buffer has been interpreted as a kind of crystallization at the interface,[31] with the size of the critical nucleus estimated to be of the order of 5 to 10 molecules.[31]

$SCN^-$ ions are well known for their ability to crystallize HEWL at acidic pH.[16,17] Moreover, many proteins are known to have a strong affinity for thiocyanate ions,[28] hence, at the high concentrations of protein close to the interface, the $SCN^-$ ions may interact strongly with the proteins. This has been demonstrated at pH 4.75 in acetate buffer[16,17] but no direct proof is available at the moment at the pH of our experiments.

Further work would also need to investigate the influence of the thiocyanate concentration on the observed process and provide a complete description of the adsorption kinetics with a mathematical model combining the two principal characteristics we identified from our experiments, namely the presence of an inflexion point, attributed to efficient adsorption on the deposited nuclei and saturation at a coverage close to what is predicted for a monolayer, attibuted to a surface exclusion phenomenon between the growing clusters.

In this work we have described the occurrence of the lag phases (Fig. 1) in terms of the time needed to reach the critical nucleus size in solution before the onset of fast adsorption. However, our preparation of the mother protein solution from the lyophilized powder and the small time allowed for equilibration of the diluted HEWL solution before the beginning of the adsorption experiment may hinder complete hydration of the protein and hence could be the source of an alternative explanation for the observed phenomenology. Indeed effects rationalized by means of the Hofmeister series are strongly related to biopolymer hydration.[10,11] The question of the hydration and structure of HEWL in the presence of $SCN^-$ anions will also be considered in our forthcoming studies.

## Acknowledgements

We thank the Ciba Geigy Jubilee Foundation for financial support and one of the anonymous referees for stimulating discussions about hydration and its effects on the physical and biological properties of proteins.

## References

1 V. Ball and J. J. Ramsden, *J. Phys. Chem. B*, 1997, **101**, 5465.
2 P. Schaaf and J. Talbot, *J. Chem. Phys.*, 1989, **91**, 4401.
3 J. J. Ramsden, 1998, in *Biopolymer at Interfaces, Surfactant Science Series*, ed. M. Malmsten, Marcel Dekker, New York, vol. 75, ch. 10, pp. 321–361.
4 C. M. Roth and A. M. Lenhoff, *Langmuir*, 1995, **11**, 3500.
5 M. R. Bruzzesi, E. Chiancone and E. Antonini, *Biochemistry*, 1965, **4**, 1796.

6 R. C. Deonier and J. W. Williams, *Biochemistry*, 1970, **9**, 4260.
7 A. Ball and R. A. L. Jones, *Langmuir*, 1995, **11**, 3542.
8 J. J. Ramsden and J. E. Prenosil, *J. Phys. Chem.*, 1994, **98**, 5376.
9 R. Kurrat, J. E. Prenosil and J. J. Ramsden, *J. Colloid Interface Sci.*, 1997, **185**, 1.
10 K. D. Collins and M. W. Washabaugh, *Q. Rev. Biophys.*, 1985, **18**, 323.
11 M. G. Cacace, E. M. Landau and J. J. Ramsden, *Q. Rev. Biophys.*, 1997, **30**, 241.
12 C. T. Shibata and A. M. Lenhoff, *J. Colloid Interface Sci.*, 1992, **148**, 469.
13 C. T. Shibata and A. M. Lenhoff, *J. Colloid Interface Sci.*, 1992, **148**, 485.
14 J. J. Ramsden, *Q. Rev. Biophys.*, 1994, **27**, 41.
15 C. A. Haynes and W. Norde, *J. Colloid Interface Sci.*, 1995, **169**, 313.
16 M. M. Riès-Kautt and A. F. Ducruix, *J. Biol. Chem.*, 1989, **264**, 745.
17 M. M. Riès-Kautt and A. F. Ducruix, *J. Crystal Growth*, 1991, **110**, 20.
18 C. R. Cantor and P. R. Shimmel, 1980, *Biophysical Chemistry*, W. H. Freeman, New York, vol. II, ch. 11.
19 P. A. Charlwood, *J. Am. Chem. Soc.*, 1957, **79**, 776.
20 Y. Harpaz, M. Gerstein and C. Chothia, *Structure*, 1994, **2**, 641.
21 V. Ball and J. J. Ramsden, *Biopolyers*, 1998, **45**, 489.
22 P. P. Herrmann and D. Wildmann, *IEEE J. Quantum Electron.*, 1983, **19**, 1735.
23 N. Goutev, Zh. S. Nickolov and J. J. Ramsden, *J. Raman Spectrosc.*, 1996, **27**, 897.
24 K. Tiefenthaler, *Adv. Biosensor*, 1992, **2**, 261.
25 K. Tiefenthaler and W. Lukosz, *J. Opt. Soc. Am. B*, 1989, **6**, 209.
26 T. W. Healy and L. R. White, *Adv. Colloid Interface Sci.*, 1978, **9**, 303.
27 Y. G. Berube and P. L. De Bruyn, *J. Colloid Interface Sci.*, 1968, **27**, 305.
28 T. Arakawa and S. N. Timasheff, *Biochemistry*, 1982, **21**, 6545.
29 J. J. Ramsden, *J. Stat. Phys.*, 1993, **73**, 853.
30 B. Mutaftschiev, 1993, in *Handbook of Crystal Growth*, ed. D. T. J. Hurle, North Holland, Amsterdam, vol. 1a, pp. 187–247.
31 B. D. Fair and A. M. Jamieson, *J. Colloid Interface Sci.*, 1980, **77**, 525.

*Paper 9/03246K*